

## التحليل الإستاتيكي للاخطى للمباني الخرسانية المسلحة دراسة حالة زلزال القاهرة

\*أمين عبد الحميد و\*\*،\* سيد محمود

\*كلية هندسة المطرية جامعة حلوان القاهرة مصر

\*\*قسم الهندسة الإنشائية كلية الهندسة جامعة الدمام المملكة العربية السعودية

### الخلاصة

في أكتوبر 1992، ضرب زلزال مدمر مدينة القاهرة مسببا أثارا ضارة في المباني الخرسانية المسلحة ويتراوح الضرر من ضرر يمكن إصلاحه الى ضرر يؤدي الى الإنهيار التام. وهذا أدى إلى الإهتمام للتعرف على الكيفية التي تتصرف بها المباني الخرسانية أثناء حدوث الزلازل. هذا البحث يعرض من خلال المحاكاة العددية التحليل الإستاتيكي للاخطى لتقييم الاداء المتوقع لمبنى سكنى من الخرسانة المسلحة مكون من 12 طابقا ويتكون نظامه الإنشائي من الإطارات المقاومة للعزوم ويقع المبنى فى مدينة القاهرة. لهذا الغرض تم إستخدام برنامج الإيتابس (ETABS) لعمل نمذجة للمبنى وتحليله باستخدام التحليل الإستاتيكي للاخطى (PUSHOVER). فى البداية تم إجراء التحليل تحت تأثير الأحمال الإستاتيكية المكافئة، ومن ثم تم إجراء التحليل الإستاتيكي الغير خطى وفقا لأوصت به الكودات العالمية والمراجع المختصة بالتقييم الزلزالى مثل ATC 40 وذلك تحت تأثير مستويين مختلفين من الهزات الارضية وفى إتجاهين متعامدين. أظهرت نتائج الدراسة ان المباني المُصممة بشكل صحيح تؤدي وبشكل جيد تحت تأثير الاحمال الزلزالية التي تتعرض لها مدينة القاهرة ومن الواضح أيضا أن المنشأ الحالي يتصرف بشكل مماثل لآلية نظام الكمر الضعيف مع العمود القوي. ومع ذلك وتحت تأثير الأحمال الزلزالية الغير المتوقعة والمخصصة لمدينة القاهرة، تظهر المفاصل اللدنة فى مستوى خطر وفقا لتصنيف ATC 40 وهي بحاجة الى تقوية نتيجة الضرر. فى حالة إذا كان التصميم غير كافى لمقاومة قوى القص، ستتكون المفاصل اللدنة نتيجة لقوى القص ويكون الانهيار الغير مرن هو المسيطر على السلوك الغير مرن.

# **Nonlinear static analysis of reinforced concrete framed buildings - A case study on Cairo earthquake**

Ayman Abd-Elhamed\* and Sayed Mahmoud\*\*,\*

*\*Faculty of Engineering at Mataria, Helwan University, Cairo, Egypt*

*\*\*Department of Construction Engineering, College of Engineering, University of Dammam, Saudi Arabia*

*\*\*Corresponding author: elseedy@hotmail.com*

## **ABSTRACT**

On October 1992, a devastating earthquake struck Cairo, causing detrimental effects in reinforced concrete (RC) buildings ranging from repairable damage to total collapse. Considerable attention has been paid in order to explicitly evaluate how RC buildings are likely to perform during earthquakes. This paper presents, through numerical simulations, a nonlinear static analysis to assess the performance of a residential 12-storey RC moment-resisting-frame building located in Cairo. The well-known software package ETABS is used for implementing the framed building model and performing the pushover analysis. The analysis is first performed under equivalent static force technique as a primary step. In the second and main step of analysis, the nonlinear static pushover analysis is performed following the ATC 40 procedures in assessing the performance of the framed building under two different levels of shakings. The pushover analysis is carried out in both x and y-directions. The results of the study showed that properly designed buildings perform well under seismic load level that fits Cairo zone, where the building clearly behaves like strong column-weak beam mechanism. However, when unexpected seismic load of peak acceleration exceeds that for Cairo, the building seems to be vulnerable and need to be strengthened where the formed plastic hinges appear in dangerous levels. For buildings inadequately designed against shear, the plastic hinges formed due to shear have been found to cause a non-ductile failure even under the level of shaking that fits Cairo zone.

**Keywords:** Egyptian code; performance levels; performance point; pushover analysis; RC framed building.

## **INTRODUCTION**

Normally, the preliminary design of civil engineering structures is typically based on the traditional force based design procedures, which are used to judge performance

of structures. These methods are specified by the governing building codes. Structures under strong ground motions behave in an inelastic way keeping some levels of damage and cracks instead of remaining elastic, which is cost effective from design point of view. The recent advent of structural design performance for a particular level of earthquake, such as displacement based Seismic design (DBSD) (Moehle, 1992 & Priestley *et al.*, 2007 & Benedetti *et al.*, 2008) is broadly defined as any seismic design procedure in which displacement related quantities are used to evaluate performance of structure. The DBSD method has been developed to have the ability to overcome the disadvantages of the other comparable methods especially the conventional force based design technique (Della Corte *et al.*, 2007). Moreover, the DBSD method has been applied for different types of structures (Shedid & El-Dakhkhni, 2014; Ahmadi *et al.*, 2015; Mergos & Beyer, 2015). The major difference between DBSD and force based design techniques in performance evaluation of structures is the use of peak displacement response of the equivalent single-degree-of-freedom (SDOF) instead of elastic characteristic of the building system. Currently, nonlinear static analysis can be carried out using two available procedures namely; (i) displacement coefficient method (DCM), which is included in FEMA-356 package (Federal Emergency Management Agency, 2000), (ii) capacity spectrum method (CSM), which is included in the ATC-40 package (Applied Technology Council, 1996; Fajfar, 1998; Freeman, 1998). It is worth noting that both of the aforementioned procedures predict the structural demands through similar performance based engineering techniques that mainly depend on the nonlinear static analysis.

The process of displacement spectrum can easily replace the elastic acceleration spectrum. This may be due to the damage of structures under earthquake loads certainly defined in terms of curvatures, rotations of members and drifts at storey levels, which specifically represent the structural deformations. One of the simplest ways to calculate such displacement spectra  $SD$  is through converting the absolute acceleration spectra  $SA$  for all natural periods  $T$  following the relation:

$$SD = SA \left( \frac{T}{2\pi} \right)^2$$

The figure below show the acceleration response spectrum curves and the corresponding displacement curves for earthquake records scaled to 0.15g to meet the peak ground acceleration of Cairo zone. Moreover, curves are plotted with different values of damping ratios.

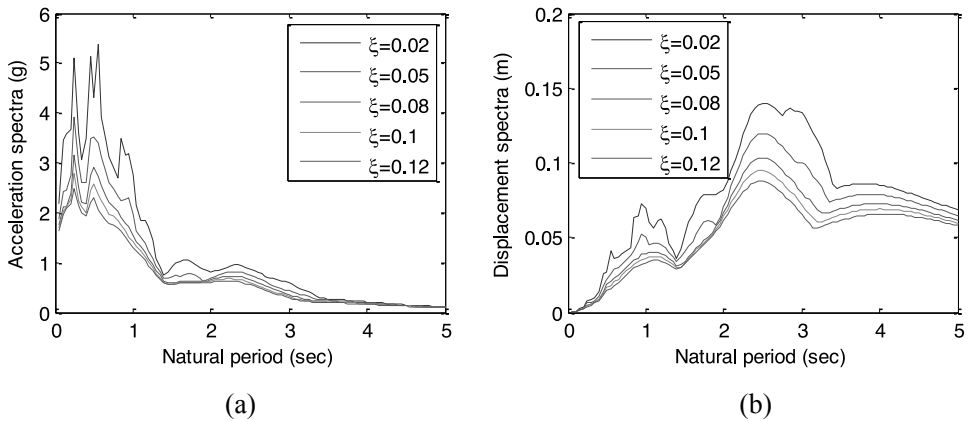


**Fig. 1.** Response spectrum curves for different damping ratios versus structure natural periods (a) Acceleration spectra (b) Displacement spectra

Both FEMA-356 and ATC-40 packages are mainly based on creating of a pushover curve in order to capture the inelastic force-deformation behavior. However, for a given ground motion, FEMA-356 and ATC-40 use different ways to calculate the global inelastic displacement demand. This curve is useful in ascertaining the capability of a structure to sustaining certain levels of seismic loads (Habibullah & Pyle, 1988; Fajfar, 2000; Lakshmanan, 2006; Kadid & Boumrkik, 2008).

The Egyptian code provides static and dynamic approaches for analysis and seismic design against earthquake load (Abdel-Raheem *et al.*, 2013; Abdel-Raheem, 2011). The static approach includes the method of equivalent static force. However, the dynamic approach includes two methods namely; the response spectrum method and the method of time-history analysis. The equivalent static force method is limited to specified structures in terms of symmetry, rigidity and regularity of the structure. However, the response spectrum analysis method is applicable for all types of structures, where it overcomes the disadvantages related to the static method. Similar to the dynamic response spectrum analysis, the dynamic time-history analysis method can be applied to any type of structure. In addition, this method provides the highest accuracy among the other two methods. However it is considered as cost effective. Independently of the seismic design procedure used, a minimum base shear force must be considered in determining the design shear force at the base of the building. For comparison purposes, the national building code of Canada (NBCC) approved the dynamic analysis to be the default analysis method for seismic design. For only specific cases, the NBCC allow designers to use the traditional lateral static force method (Boivin & Paultre, 2010).

This study is carried out to discuss the performance of a 12-storey RC building located in Cairo. The considered building is designed according to the Egyptian code

(ECP-201, 2008) and subjected to seismic hazard of Cairo zone as well as earthquake records beyond the ones predefined by Egyptian code for loads. Investigation of shear failure due to formation of shear hinges, considering the designed frame building's inability to resist shear is studied. The numerical simulations are performed using ETABS V13.2.1 (ETABS User's Manual, 2013) and guidelines of ATC-40 and FEMA 356 are followed.

## **NONLINEAR STATIC PUSHOVER ANALYSIS**

The pushover analysis is a technique used to evaluate the real strength and the seismic performance of structures. The static nonlinear analysis is performed under existing vertical loads with gradually increasing defined lateral loads. Structural loading magnitude is increased in an incremental way according to a certain predefined pattern and hence the sequence of cracks, yielding, plastic hinge formations, and failure modes of the structure are found. Consequently, at each event, the structure experiences a loss in stiffness. A plot of the total base shear versus roof displacement, at the center of mass of structure, is obtained to develop a capacity curve for the structure as shown in Figure 2. The capacity curve produces a target displacement equivalent to the one that will be created under the design earthquake. The pushover analysis allows loading the structure up to failure; thus it can be considered as a procedure for estimating both collapse load and ductility capacity. The ATC-40 and FEMA-356 documents have developed modeling parameters, acceptance criteria and procedures of pushover analysis.

There are two trends that may be used in performing pushover analysis. The first one, sometimes called force control trend, calculates the incremental displacements of the considered structures due to exposing the structure to incremental lateral forces. Contrary to the first trend, in the second trend, i.e., deformation control trend, the structure is subjected to a deformation profile, and the required lateral forces to induce those deformations are computed. However, the force control trend is highly recommended in performing analysis, compared to the one with deformation control, since the deformation profile is unknown.

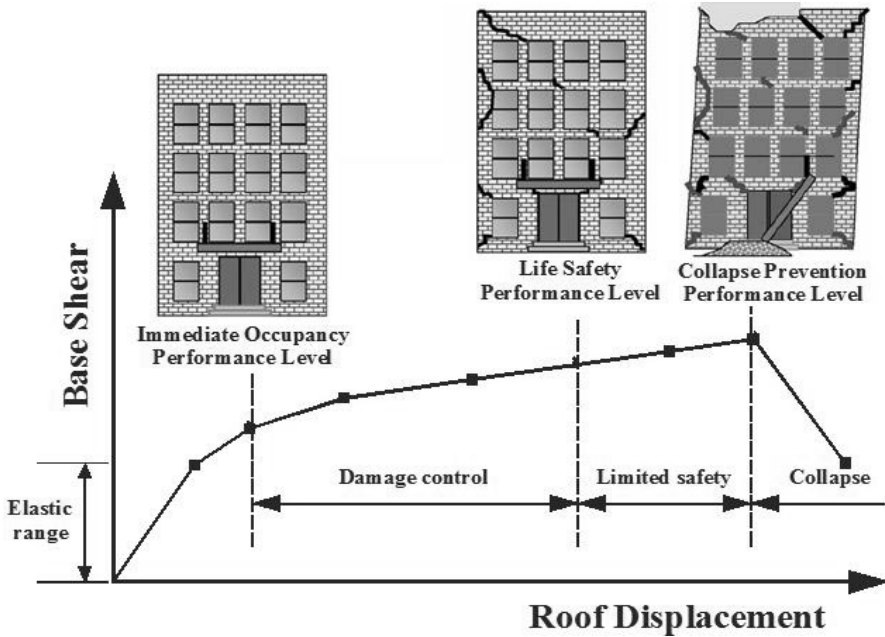
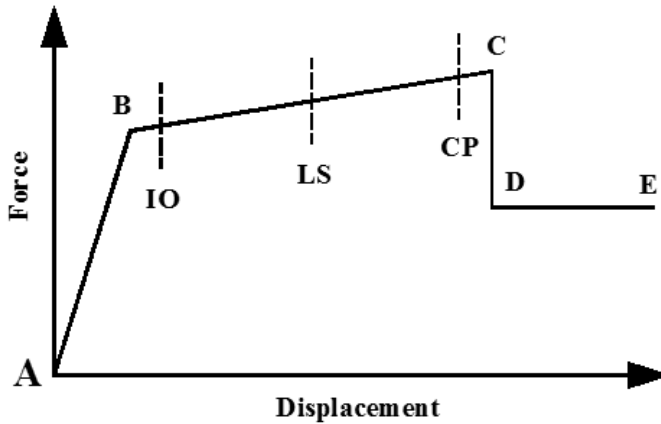


Fig. 2. Capacity curve of structures with illustration of building performance levels and damage states

### ACCEPTANCE CRITERIA (PERFORMANCE LEVELS)

When a concrete element undergoes large deformations in the post-yield stage, it is assumed that the entire deformation takes place at a point called “plastic hinge” used in pushover analysis. As shown in Figure 3, five points labeled A, B, C, D, and E define the force deformation behavior of a plastic hinge. Point A is the origin, B is the yield point, C is the ultimate point and points D and E are measures of residual strength and displacement capacity. Three points labelled immediate occupancy (IO), life safety (LS) and collapse prevention (CP) are used to define the acceptance criteria for the plastic hinge as per FEMA and ATC 40.

IO as one of the performance levels refers to a very light overall damage to the building. In addition, the strength and stiffness remain nearly as those of pre-earthquake loading. Claddings and ceilings as nonstructural elements together with the mechanical and electrical components remain secured as well. LS level is characterized with (i) a significant structural and nonstructural damage, (ii) substantial amounts of building strength and stiffness are lost compared with pre-earthquake lateral strength and stiffness, (iii) nonstructural components are secured and not presenting a falling hazard. The case in which the structure sustain severe damages is the CP. During the CP performance level, the lateral-force resisting system loses most of its pre-earthquake strength and stiffness and the building is near to collapse.



**Fig. 3.** Different stages of plastic hinge

## **BUILDING MODEL**

### **Geometry**

This study investigates the seismic behaviour of multi-storey reinforced concrete frame building with 12-storey for residential use. The building has 3-spans and 5-bays of 4 m in both directions as shown in Figure 4. The typical floor height is 3m, except for the first floor height, which is considered to be of 4m, which represents a typical building constructed in Cairo, Egypt. The cross sections of the columns are reduced every 3 stories towards the roof of the building, which is a common construction practice in Egypt.

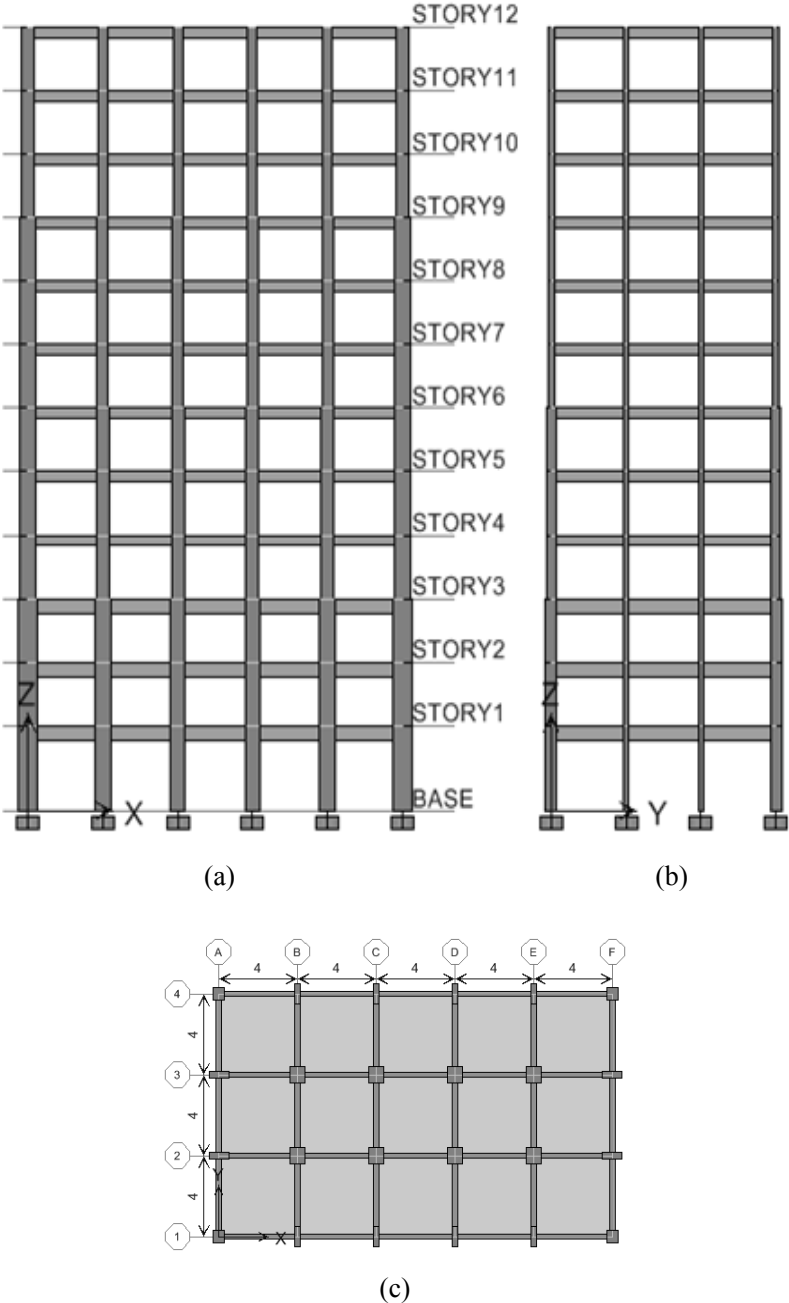


Fig. 4. Schematic representation of (a) building elevation (b) side view (c) and typical floors plan of the 12-storey framed building.

## Material properties

Concrete having a characteristic strength  $f_{cu}$  of 25 N/mm<sup>2</sup> after 28-days, and high-grade steel with yield strength  $f_y = 360$  N/mm<sup>2</sup> are used for analysis and design. The specific weight of reinforcement concrete is taken as  $\gamma_c = 25$  kN/m<sup>3</sup>, modulus of elasticity  $E_c$  is determined using the formula  $E_c = \sqrt{14000f_{cu}}$  (ECP-201, 2008). The elastic modulus of steel is taken as 210 KN/mm<sup>2</sup>. Poisson's ratios  $\nu$  of concrete and steel are taken equal to 0.2 and 0.3, respectively.

## Section properties and reinforcement details

The inner and corner columns are considered to have square cross sections. The other columns of the edge frames are considered to appear as rectangular in shape as shown in Figure 4. All columns are assumed to be fixed at the foundation level. The dimensions of all frame members are shown in Table 1. The selected reinforcement ratios for the beams are within the range allowed, where the maximum and the minimum reinforcement ratios are 1.25% and 0.3% respectively (ECP-201, 2008). For the non-ductile columns, steel reinforcement ratios have been chosen to satisfy the Egyptian code requirements in which the range allowed for maximum and minimum percentage of steel reinforcement are 4.0% and 0.8% respectively. The RC building is provided with 0.12 m thick floor slabs, which are considered as rigid floor diaphragms.

## Gravity loads

The loads that act on the RC building are categorized as gravity loads, which include dead and live loads, and lateral loads, which include earthquake loads. The assigned values for the dead loads in terms of the weight of flooring cover and the weight of partitioning elements are 1.5 kN/m<sup>2</sup>, and 2 kN/m<sup>2</sup> respectively. The own weight of the structural elements, as a part of the dead loads is automatically computed by the used structural software package. According to the Egyptian code, The live load value for residential RC building has been assigned to be 2.5 kN/m<sup>2</sup>.

**Table 1.** Dimensioning and reinforcement of building elements

Structural element		Story number			
		1, 2, 3	4, 5, 6	7, 8, 9	10, 11, 12
Beams	Cross section (m <sup>2</sup> ) Reinforcement	0.25 x 0.70 4 $\Phi$ 16	0.25 x 0.50 4 $\Phi$ 16	0.25 x 0.50 4 $\Phi$ 16	0.25 x 0.50 4 $\Phi$ 16
Edge Columns	Cross Section (m <sup>2</sup> ) Reinforcement	0.30 x 1.00 18 $\Phi$ 16	0.30 x 1.00 14 $\Phi$ 16	0.30 x 0.80 12 $\Phi$ 16	0.30 x 0.70 10 $\Phi$ 16
Inner Columns	Cross Section (m <sup>2</sup> ) Reinforcement	0.80 x 0.80 32 $\Phi$ 16	0.70 x 0.70 24 $\Phi$ 16	0.60 x 0.60 20 $\Phi$ 16	0.50 x 0.50 16 $\Phi$ 16
Corner Columns	Cross Section (m <sup>2</sup> ) Reinforcement	0.60 x 0.60 20 $\Phi$ 16	0.50 x 0.50 16 $\Phi$ 16	0.40 x 0.40 12 $\Phi$ 16	0.30 x 0.30 4 $\Phi$ 16

### **Lateral static loads equivalent to seismic loads**

The loads which are considered in the seismic design of building is the full dead loads plus 50% of the live loads (ECP-201, 2008). The seismic parameters to determine the base shear force of the building are stated in Table 2, depending on the seismic characteristics of Cairo city.

The analysis of the building has been performed using pushover analysis. Two types of loads were considered; the GRAVITY load in which the predefined vertical loads, i.e., dead and live loads are applied. PUSHX and PUSHY are the lateral loads applied in both x-direction and y-direction respectively.

**Table 2.** The seismic characteristics of the Cairo city

Response Curve	1	Importance factor $\gamma_I$	1
Number of floors	12 floors	Building location (zone)	Zone (3)
Typical floor height	3 m	Damping correction factor $\eta$	1
Ground floor height	4 m	Response modification factor R	5
Typical floor weight	277 ton	Soil type	Soil C
Ground floor weight	277 ton	Ct factor	0.075

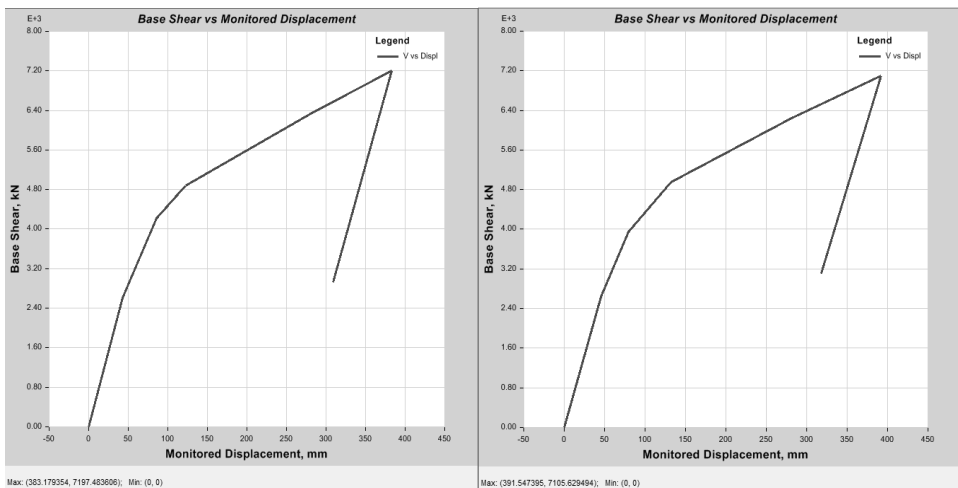
### **RESULTS OF ANALYSIS**

The adopted multi-storey reinforced concrete frame building model introduced in the previous section is used in the nonlinear static analysis. Pushover analysis scheme in which the dynamic imposed loads are incrementally applied to structural model are utilized in a step by step way. The ETABS software package is used to perform the simulation analysis using ground acceleration of intensities of 0.15 g and 0.3 g in x-direction and y-direction considering an adequate shear design frame building so as to allow flexural failure or ductile failure instead of the undesired shear failure. The building model is changed later from adequate shear design frame building to inadequate one in order to examine the effect of shear hinge formation on the response of the buildings. The results for two different types of building frame, namely, adequate shear design and inadequate shear design frame buildings are presented in the coming sub-sections in the form of figures and tables. The trends observed in the results are also discussed in these sub-sections.

#### **Flexural failure analysis**

This subsection presents the results from analysis of the adequate design building against shear, where ductile failure due to the formation of flexural plastic hinges is expected under applied earthquake loads of intensity 0.15 g and 0.3 g in x-direction

and y-directions. The pushover curves for load versus deflection due to the application of lateral load in x- and y-directions are presented in Figure 5. The plotted curves seem to be identical although the direction of loading is different. The curves start with a linear portion followed by nonlinearity due to the inelastic action of beams and columns. From the analysis, it has been found that the captured roof displacement and base shear in x-direction are 383 mm and 7198 kN respectively. The analysis in y-direction shows roof displacement and the corresponding base shear of 391 mm and 7105 kN respectively.



(a)

(b)

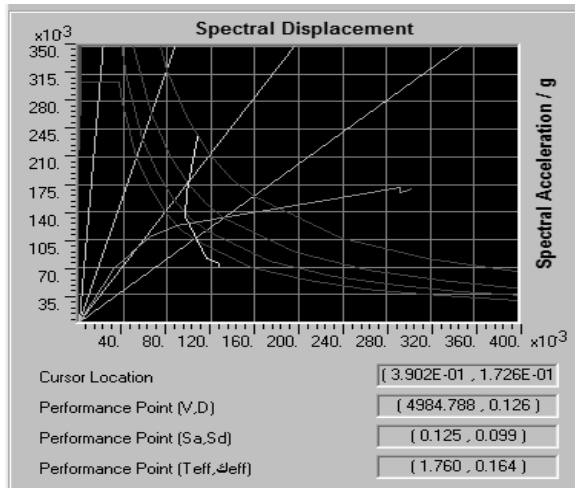
Fig. 5. Pushover curve: (a) loading in x-direction (b) loading in y-direction

### Pushover results (x-direction)

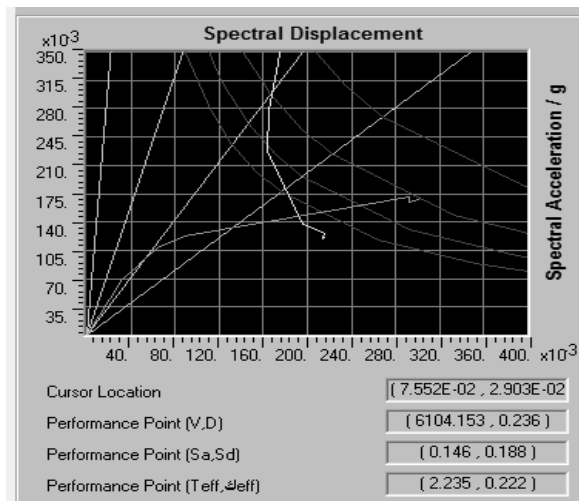
The pushover curves and performance points obtained by superimposing the demand spectrum curve and the ATC-40 capacity spectrum curve under the considered two levels of shaking, 0.15 g and 0.3 g, are presented in Figure 6. Figure 6(a), presents the results due to the application of shaking earthquake of intensity 0.15g in x-direction. The chosen 0.15 g intensity is coinciding with Cairo zone intensity. The seismic coefficients  $C_a$  and  $C_v$  are acceleration-based and velocity-based site coefficients, respectively. Both site coefficients represent the amplification of seismic motions due to ground conditions and mainly depend on the seismic zone as well as the soil type at the site (Sobaih, 1996; Mohamed *et al.*, 2012 ).

The PGA considered herein is of intensity 0.15 g and the type of soil at the site is very dense. These known values of regional seismicity and soil condition at the site control the assigned values to the seismic coefficients  $C_a$  and  $C_v$  to be of 0.22 and 0.32 respectively. The performance point, at which the capacity and demand curves meet,

has been found to be associated with an inelastic roof displacement of 0.125 m. For the same level of shaking, i.e., 0.15 g, and at the same specified performance point, an effective natural period  $T_{eff}$  of 1.760 sec has been obtained (see Figure 6(a)). On the other hand, for level of shaking of 0.3 g, which exceeds that specified for Cairo zone, the assigned values for the used seismic coefficients  $C_a$  and  $C_v$  are 0.36 and 0.54 respectively. A higher effective natural period  $T_{eff}$  of value 2.235 sec has been obtained as can be seen in Figure 6(b). The performance point has been assigned at an inelastic roof displacement of 0.236 m.



(a)



(b)

Fig. 6. Pushover curve, demand spectrum and performance point under applied acceleration of (a) 0.15 g (b) 0.3 g in x-direction.

Table 3 presents the pushover results in x-direction in terms of the number of steps required to push the building model till failure or reaching a target displacement of about 4% of the building height as recommended by the design codes. The corresponding displacements and base shear at each step are presented in the table. The number of plastic hinges formed at each performance level stage is presented in Table 3 as well. The pushover analysis results for the shaking of intensity 0.15 g in x-direction can be obtained from the table with the use of Figure 6(a) where the performance point recorded at roof displacement of about 0.126 m. From Table 3, the pushing step at which nearest roof displacement to the one recorded at the performance point can be found at step 3. At this step it can be seen that at the performance point, where the capacity and demand curves meet, out of 1488 of the assigned plastic hinges, about 1136 are formed in A-B stage. The remaining assigned numbers of plastic hinges are 104, 148, 100, and 0 and respectively found in B-IO, IO-LS, LS-CP and CP-C stages. Table 3 confirms that plastic hinges formed beyond CP stage are zero. The overall performance of building acts like LS to CP following the locations and numbers of the aforementioned formed plastic hinges.

In this event, the formation of plastic hinges causes decrease in both structure rigidity and original strength, followed by damage of some structural elements and components. Plastic hinges formations for the building mechanisms at different levels have been obtained in Figure 7 for 0.15 g PGA intensity. The formation starts with beam ends and base columns of lower stories, and then propagates to the upper stories. As it can be seen from the figure, the failure mechanism is of the desirable kind. This is consistent with the known philosophy, which suggests, “strong column and weak beam” (when their strengths are compared).

Moving to the 0.3 g acceleration level of loading, it can be seen from Figure 6(b) that the roof displacement at the performance point is 0.236 m. Step 4 in Table 3 provides a value of 0.2728 for the roof displacement and can be considered as the nearest value to the one recorded at the performance point. This captured roof displacement at the pushing step 4 is higher than the one at the performance point, which means that the demand curve intersects with the capacity curve beyond CP stage and hence the structure deformed beyond ductile limit and can experience instability and may collapse. As it can be seen from the table at step 4, out of the 1488 assigned plastic hinges, about 1110 were in A-B stage, 92, 72, 212, 0, and 2 hinges are in B-IO, IO-LS, LS-CP, CP-C and C-D stages respectively.

**Table 3.** Pushover result (x-direction loading)

step	Displacement	Base Force	A-B	B-IO	IO-LS	LS-CP	CP-C	C-D	D-E	>E	TOTAL
0	0.0000	0.00	1484	4	0	0	0	0	0	0	1488
1	0.0430	2655.66	1298	190	0	0	0	0	0	0	1488
2	0.0847	4264.26	1218	270	0	0	0	0	0	0	1488
3	0.1135	4853.75	1136	104	148	100	0	0	0	0	1488
4	0.2728	6479.24	1110	92	72	212	0	2	0	0	1488
5	0.3639	7268.23	1108	94	72	210	0	0	4	0	1488
6	0.3639	7036.75	1106	96	72	210	0	0	4	0	1488
7	0.3638	7147.58	1098	104	68	210	0	4	4	0	1488
8	0.3767	7258.92	1098	104	68	200	0	6	12	0	1488

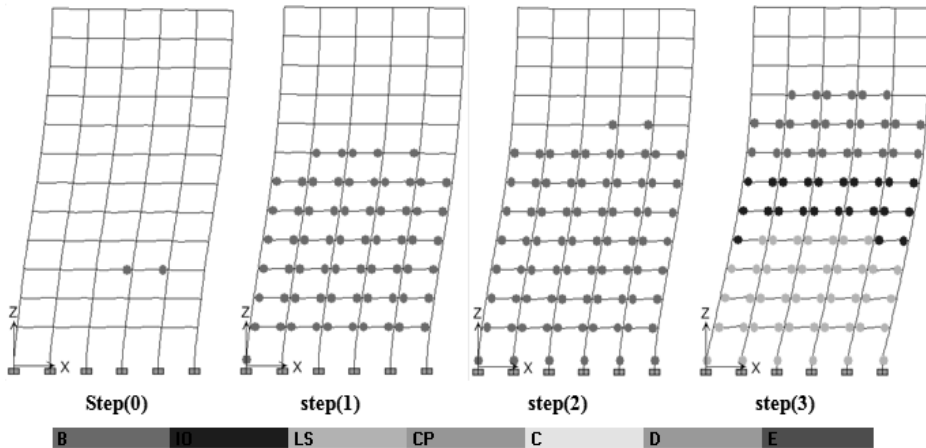


**Fig. 7.** History of formation of plastic hinges under 0.15 g acceleration in x-direction.

Plastic hinges formation for the building mechanisms under 0.3 g earthquake intensity are illustrated in Figure 8. The formation starts with beam ends and base columns of lower stories, and then propagates to the upper stories. As it can be seen from the figure, the failure mechanism is not of the desirable kind where the lower columns yields exceeding collapse condition C.

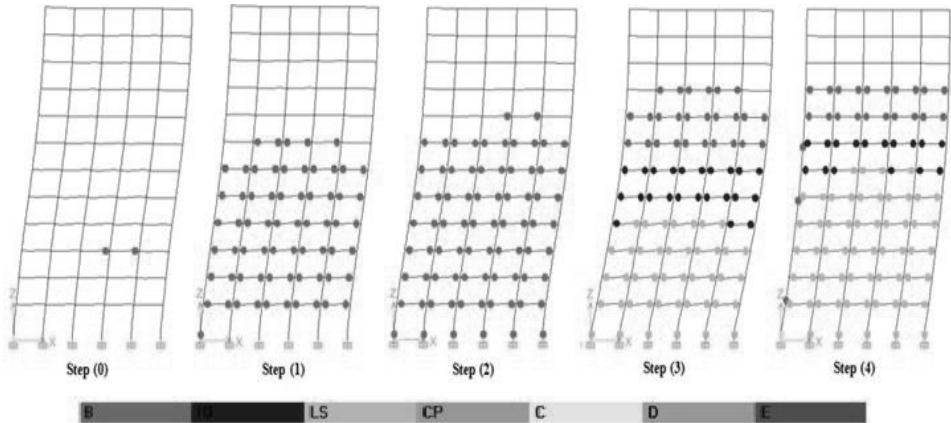


**Fig. 8.** History of formation of plastic hinges under 0.3 g acceleration in x-direction.

### Pushover results (y-direction)

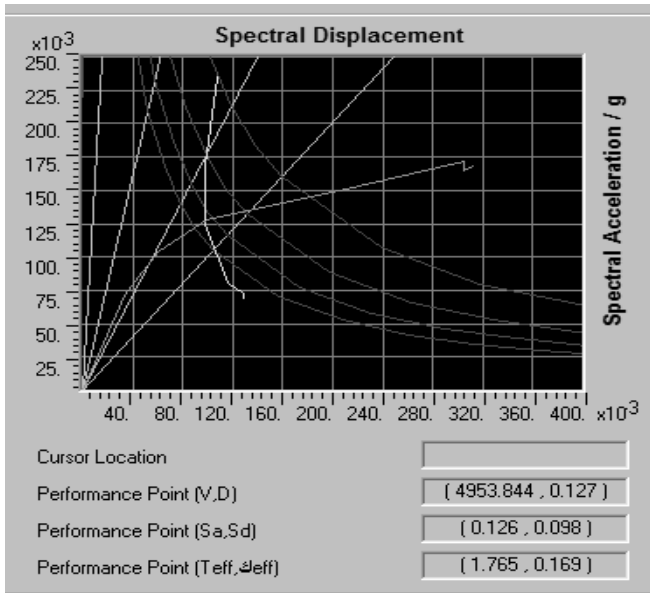
The obtained results of the pushover analysis for the reinforced concrete framed building under the considered two levels of shaking, 0.15 g and 0.3 g in y-direction show similarity to those obtained for x-direction loading case. Figure 9 presents the induced performance point under the application of shaking earthquake of intensity 0.15g (see Figure 9(a)) and 0.3g (see Figure 9(b)). The performance points for 0.15 g and 0.3 g intensities have been found to be associated with inelastic roof displacements of 0.127 m and 0.238 respectively. The aforementioned values of roof displacement respectively show percentage increase of about 12.4% and 2.25% compared to the obtained values for loading in x-direction with the intensity levels 0.15 g and 0.3 g respectively. The corresponding effective natural periods are of 1.765 sec and 2.234 sec.

The pushover results for the shaking intensities of 0.15 g and 0.3 g in terms of acceptance criteria and performance levels can be seen in step 3 and step 4 which respectively appear in Table 4, where the captured roof displacements at step 3 and step 4 has been found to be 0.1296 and 0.2791 respectively. These assigned values are considered as the nearest to the inelastic roof displacements captured at the performance point. In comparison to x-direction results presented in Table 3, it has been found that the values of shear at base increase with about 3% for level of shaking 0.15g. However, the shear value under the application of 0.3g level of intensity has been decreased with about 1.3%. Insignificant changes in the assigned plastic hinges formed during B-IO, IO-LS, LS-CP and CP-C stages have been found for the two levels of shaking is comparable with the formed plastic hinges under x-direction loading (compare Table 3 and Table 4, Figures 7 and Figure 10, Figure 8 and Figure 11). Hence, the overall performance of building loaded with earthquake

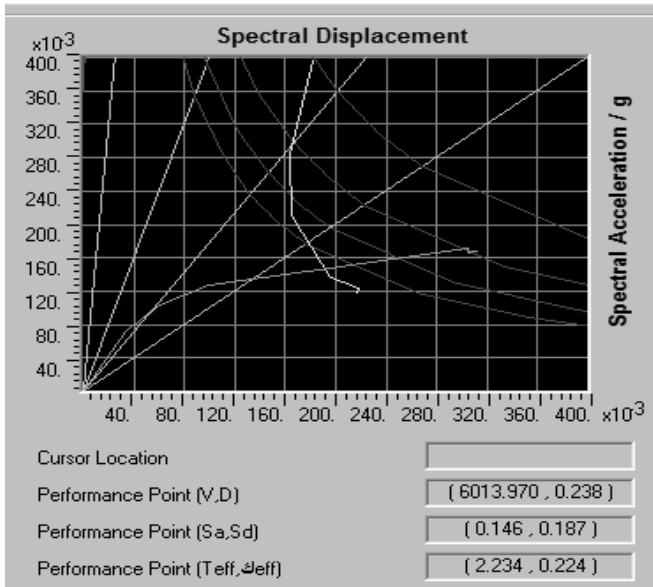
intensity of 0.15 g in y-direction acts like LS to CP and the failure mechanism is of the desirable kind. For 0.3 g acceleration level of loading the failure mechanism is also similar to the mechanism obtained in x-direction where the lower columns yield exceeding collapse condition C.

**Table 4.** Pushover result (y-direction loading)

step	Displacement	Base Force	A-B	B-IO	IO-LS	LS-CP	CP-C	C-D	D-E	>E	TOTAL
0	0.0000	0.00	1484	4	0	0	0	0	0	0	1488
1	0.0449	2679.39	1314	174	0	0	0	0	0	0	1488
2	0.0800	4029.78	1220	268	0	0	0	0	0	0	1488
3	0.1296	5001.81	1152	104	118	114	0	0	0	0	1488
4	0.2791	6397.16	1118	104	62	202	0	2	0	0	1488
5	0.3842	7260.97	1118	104	62	198	0	0	4	0	1488
6	0.3842	7006.95	1116	106	62	198	0	0	4	0	1488
7	0.3887	7095.37	1114	106	64	194	0	4	4	0	1488
8	0.3942	7157.90	1114	106	64	190	0	6	12	0	1488



(a)



(b)

**Fig. 9.** Pushover curve, demand spectrum and performance point under applied acceleration of (a) 0.15 g (b) 0.3 g in y-direction.

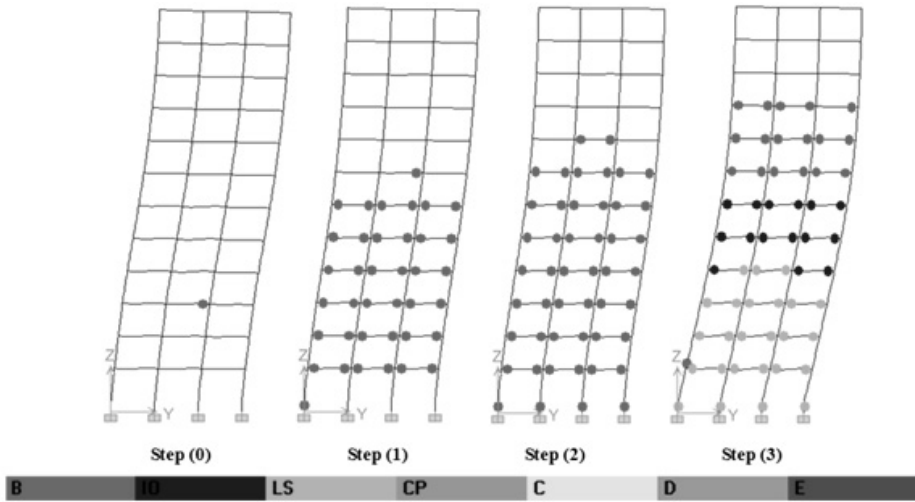


Fig. 10. History of formation of plastic hinges under 0.15 g acceleration in y-direction.

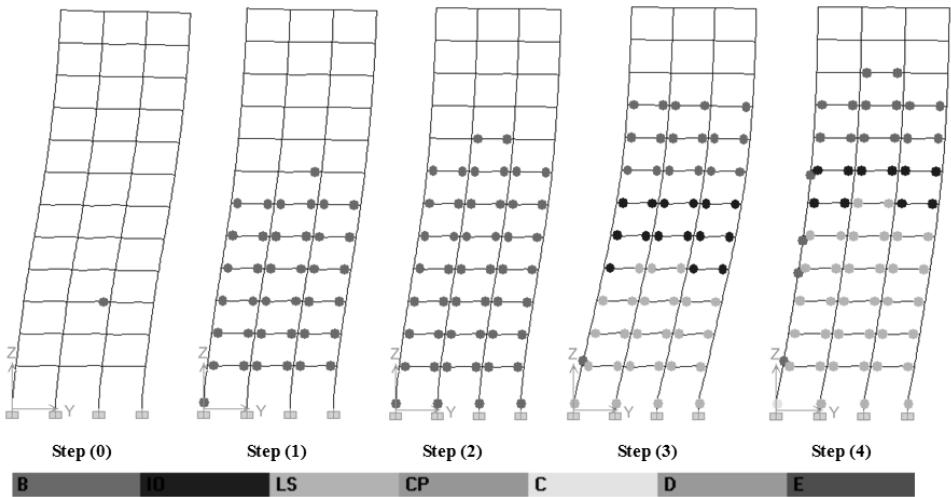


Fig. 11. History of formation of plastic hinges under 0.3 g acceleration in y-direction.

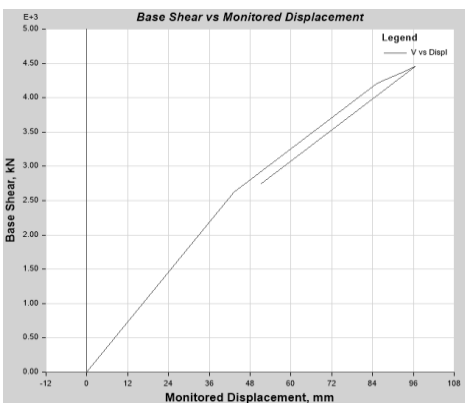
### Shear failure analysis

The reinforced concrete frames with weaker columns suffer brittle shear and axial failure, while the stronger beams remain elastic. This undesirable behavior is also seen in the 2011 Simav earthquake (Yılmaz & Avsar, 2013). Figure 12 shows columns failure in a building with strong beams and weak columns.

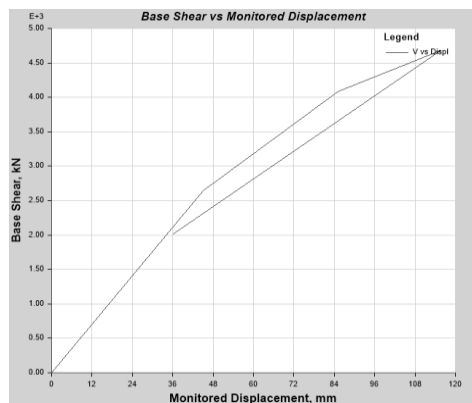


Fig. 12. Columns failure in a building with strong beams and weak columns.

It is known that shear failure occurs due to inadequate shear design. However, the design codes provide regulations and specifications that ensure ductile detailing reinforcement for the ultimate moment capacity level and the corresponding adequate shear reinforcement. This allows buildings to have the recommended flexural failure or ductile failure instead of the undesired shear failure. This section presents the effect of shear hinges formation on the response of the buildings through analysis of an inadequately designed frame building against shear and subjected to earthquake of intensity 0.15 g in x-direction and y-direction.



(a)



(b)

Fig. 13. Pushover curve: (a) loading in x-direction (b) loading in y-direction

The pushover curves for load versus deflection due to the application of lateral load in x- and y-directions are presented in Figure 13 for building model with shear hinges. The plotted curve for x-direction loading seems to be different from the plotted pushover curve from y-direction loading (compare Figure 13(a) and 13(b)). The curves start with a linear portion followed by nonlinearity due to the inelastic action of beams and columns. From the analysis, it has been found that the captured roof displacement and base shear in x-direction are 383 mm and 7198 kN respectively. The analysis in y-direction shows roof displacement and the corresponding base shear of 391 mm and 7105 respectively.

As it can be seen from the figure, the two pushover curves for x and y-directions follow the linear state, even after the beams and columns undergo inelastic deformations. However, the inclination gets smaller as the building attains deformations. Comparing the pushover curves presented in Figure 13 with those presented in Figure 5 for the flexural failure case shows significant changes. The Figures clearly show that occurrence of shear failure underestimate the obtained roof displacement and the corresponding base shear. From the analysis, it has been found that the captured roof displacement and base shear in x-direction for the case of plastic hinges formation due to shear are 96.58 mm and 4453 kN respectively. From percentage point of view, and retrieving the values of roof displacement and base shear at flexural failure clearly emphasis that an increase in both roof displacement and base shear of about 296% and 62% respectively as compared to corresponding values obtained from shear failure case. Similarly, the analysis in y-direction shows an increase in both roof displacement and base shear of about 238% and 52% respectively as compared to the values assigned at the shear failure case.

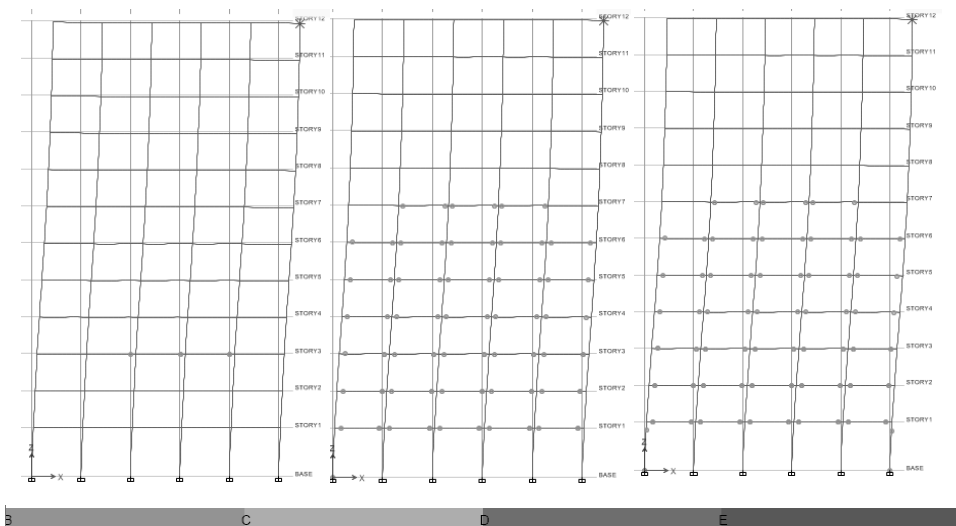


**Fig. 14.** History of formation of shear hinges under 0.15 g acceleration in x-direction.

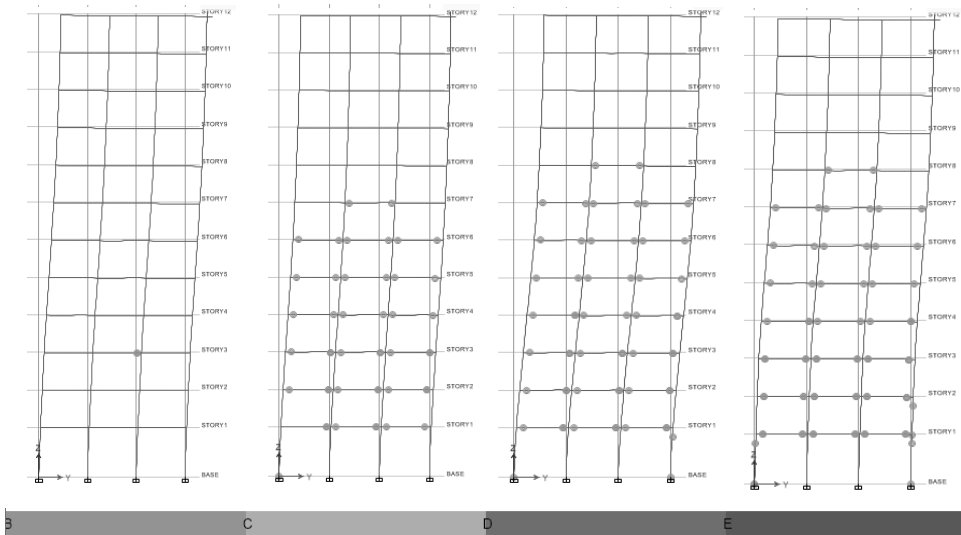


**Fig. 15.** History of formation of shear hinges under 0.15 g acceleration in y-direction.

Plastic hinges formations due to shear are presented in Figures 14 and 15 for applied earthquake load in x-direction and y-direction respectively. As it can be seen from the figures, the plastic hinges start to occur in beam ends and then the formation of these hinges starts at columns of lower levels before they extend to the upper level columns. The results from this analysis reveal the importance of designing buildings against shear failure in seismic design, otherwise a non-ductile failure of the buildings can be expected.

Based on the analysis results presented previously, the overall seismic performance of the structure in flexure under possible design-level ground motions is of good flexural performance. This may be due to the adequate prevention of unintended plastic hinges formation in beams and columns under flexural. This suggests that the proposed design method by the Egyptian design code for flexural strength is adequate. Despite the predicted good flexural performance of the structure, the predicted shear demand for the design level excitation significantly exceeds the suggested design shear envelope. This leads to a potential shear failure, which would prevent the whole structure from laterally deforming in a ductile manner. In such cases, the seismic performance of the structure might be closer to extensive damage than what is predicted in flexure. It is recommended that the current design practice code to account for such increase in shear which may be due to torsion or any other effects.

## CONCLUSIONS

In this paper, performance of a residential 12-storey RC framed building, designed in accordance with the Egyptian code for loads has been investigated considering two

levels of shakings using pushover analysis. One of the chosen levels fits the seismicity of Cairo zone and the other level is of higher magnitude. The analysis has been carried out using ETABS software tool in both x and y-directions. It has been found from the analysis using level of shaking of intensity 0.15 g applied in either x-directions or y-direction that the demand curve intersects the capacity curve near the elastic zone. Consequently the formed plastic hinges are always away from critical levels of performance and ensure that the building behaves like the strong column-weak beam mechanism which indicates that proposed model for nonlinear static analysis has produced satisfactory behavior, better seismic performance and capability to sustain seismic loads fit code requirements. However, exposing the framed building to seismic load exceeds twice the one recommended by design code shows that the demand curve intersects the capacity curve in the inelastic zone leading to formation of plastic hinges in the dangerous level. Accordingly, the building behaves poorly and needs to be strengthened to avoid severe damage or even collapse. Moreover, the results from shear failure analysis due to formation of plastic shear hinges reveal the importance of designing buildings against shear otherwise a non-ductile failure of the buildings can be expected.

## REFERENCES

- Abdel-Raheem, K., Abdel Raheem, S., Soghair, H. & Ahmed, M. 2010.** Evaluation of seismic performance of multistory buildings designed according to Egyptian code. *Journal of Engineering Sciences, Assiut University*, **38**(2):381-402.
- Abdel Raheem, S. 2013.** Evaluation of Egyptian code provisions for seismic design of moment-resisting-frame multi-story buildings. *International Journal of Advanced Structural Engineering*, **5**(20):1-18.
- Applied Technology Council, ATC-40. 1996.** Seismic evaluation and retrofit of concrete buildings, vols. 1 and 2. California.
- Benedetti, A., Landi, L. & Malavolta D. 2008.** On the design and evaluation of seismic response of RC buildings according to direct displacement-based approach. 14th World Conference on Earthquake Engineering, 14WCEE. Beijing, China, Paper No. 05-01-0424.
- Boivin, P. & Paultre, P. 2010.** Seismic performance of a 12-storey ductile concrete shear wall system designed according to the 2005 National building code of Canada and the 2004 Canadian Standard Association standard A23.3. *Canadian Journal of Civil Engineering*, **37**:1-16.
- Della Corte, G., D’Aniello, M. & Mazzolani, F.M. 2007.** Seismic design of concentrically braced steel frames: Traditional force-based vs. innovative displacement-based design approaches. Proceedings of the Third International Conference on Structural Engineering, Mechanics and Computation (SEMC 2007), Cape Town, South Africa.
- Habibullah, A. & Pyle, S. 1988.** Practical three dimensional nonlinear static pushover analysis, *Structure Magazine*.
- ETABS User’s Manual. 2013.** Integrated building design software. Computer and Structure Inc. Berkeley, USA.
- Fajfar, P. 1998.** Capacity spectrum method based on inelastic demand spectra. Report EE-3/98, IKPIR, Ljubljana, Slovenia.

- Fajfar, P. 2000.** A nonlinear analysis method for performance based seismic design. *Earthquake Spectra*, **16**(3):573–592.
- Ahmadi, F., Mavros, M., Klingner, R., Shingd, B & McLeane, D.** Displacement-based seismic design for reinforced masonry shear-wall structures. Part 1: Background and Trial Application. *Earthquake Spectra*, **31**(2):969-998.
- Federal Emergency Management Agency, FEMA-356. 2000.** Prestandard and commentary for seismic rehabilitation of buildings. Washington (DC).
- Freeman, S.A. 1998.** Development and use of capacity spectrum method. Proceedings of 6<sup>th</sup> US National Conference on Earthquake Engineering, Seattle, Washington, U.S.A., Paper No. 269.
- Kadid, A. & Boumrkik, A. 2008.** Pushover analysis of reinforced concrete frame structures. *Asian journal of civil engineering (Building and Housing)*, **9**(1):75-83.
- Lakshmanan, N. 2006.** Seismic evaluation and retrofitting of buildings and structures. *ISSET journal of earthquake technology*, Paper No. 469, **43**(1-2):pp. 31-48.
- Mergos P. & Beyer, K. 2015.** Displacement-based seismic design of symmetric single-storey wood-frame buildings with the aid of N2 method. *Frontiers in Built Environment*, **(1)**:1-11.
- Moehle, J.P. 1992.** Displacement-Based design of RC structures subjected to earthquakes. *Earthquake Spectra*, **3**(4):403-428.
- Mohamed, A., El-Hadidy, M., Deif, A. & Abou Elenean, K. 2012.** Seismic hazard studies in Egypt *NRIAG Journal of Astronomy and Geophysics*, **1**:119-140.
- Priestley, M.J.N., Calvi, G.M. & Kowalsky M.J. 2007.** Displacement based seismic design of structures. IUSS Press, Pavia, 1st edition, pp. 670.
- Shedid, M. & El-Dakhkhni, W. 2014.** Plastic hinge model and displacement-based seismic design parameter quantifications for reinforced concrete block structural walls. *Journal of Structural Engineering*, **140**(1):04013090.
- Sobaih, M. 1996.** Seismic design criteria for Egypt. Eleventh World Conference on Earthquake Engineering, Paper No. 2158.
- The Egyptian Code for Calculation of Loads and Forces in Structural and Building Work 2008.** ECP-201, Housing and Building National Research Centre. Ministry of Housing, Utilities and Urban Planning, Cairo, Egypt.
- Yilmaz, N. & Avsar, O. 2013.** Structural damages of the May 19, 2011, Ku'tahya–Simav Earthquake in Turkey. *Nat Hazards* DOI 10.1007/s11069-013-0747-2.

*Submitted:* 17/08/2015

*Revised:* 02/12/2015

*Accepted:* 06/02/2016